

QCD-aware partonic jet clustering for truth-jet flavour labelling

Andy Buckley, Chris Pollard

School of Physics & Astronomy, Glasgow University, UK

We present an algorithm for deriving partonic flavour labels to be applied to truth particle jets in Monte Carlo event simulations. The inputs to this approach are final pre-hadronisation partons, to remove dependence on unphysical details such as the order of matrix element calculation and shower generator frame recoil treatment. These are clustered using standard jet algorithms, modified to restrict the allowed pseudojet combinations to those in which tracked flavour labels are consistent with QCD and QED Feynman rules. The resulting algorithm is shown to be portable between the major families of shower generators, and largely insensitive to many possible systematic variations: it hence offers significant advantages over existing *ad hoc* labelling schemes. However, it is shown that contamination from multi-parton scattering simulations can disrupt the labelling results. Suggestions are made for further extension to incorporate more detailed QCD splitting function kinematics, robustness improvements, and potential uses for truth-level physics object definitions and tagging.

Introduction

The rise of jet substructure methods at the LHC has prompted a resurgence in attempts to distinguish “quark” and “gluon” hadronic jets from each other, primarily for use in searches for BSM phenomena. Such attempts are primarily based on the different colour charges of quarks and gluons, with the larger C_A colour factor of the gluon associated with more jet broadening and higher constituent multiplicities than the quarks’ C_F factor.

A conceptual problem immediately arises in that colour-neutral jets cannot perfectly correspond to coloured single partons. Additionally, final-state observables do not provide unambiguous evidence for two distinct statistical populations of hadronic jets. The evaluation of q/g jet tagging methods has hence been based on use of event generators’ partonic event graphs to define the “true” jet label, typically assigning a partonic identity to each final-state truth-jet by the flavour of the highest-energy or highest- p_T parton found within a fixed angular distance of its centroid. Sometimes these labelling partons are chosen from the entire partonic event record,

including parton shower (PS) evolution; sometimes they are restricted to partons associated to the hard process matrix element (ME). The labels derived using these methods are then used to determine the efficiencies and fake rates of experimental tagging techniques. Such approaches to truth labelling have several practical and conceptual drawbacks:

- their reliance on the unguaranteed physicality of partonic event records – these are typically intended more for debugging than for robust physics analysis use, and their momenta may not have physical meaning;
- even where the parton momenta are physical in their chosen frame, it is often the case that different generations of parton evolution are represented in frames different from the lab frame relevant to final state observables;
- the potential unphysical distinction between “matrix element” and “parton shower” partons – problematic for consistency of labelling at different perturbative orders and particularly for “resummation-corrected” matrix elements such as those in the POWHEG method [1] where there is no clear kinematic distinction between ME and PS emissions.

All of these limitations and assumptions cause problems in practice, notably in the inability to use the SHERPA event generator [2] whose event record is complexified by the use of matrix-element/parton-shower merging and matching (MEPS) and a dipole shower formalism with $2 \rightarrow 3$ parton branchings [3]. More traditional parton showers, i.e. the $1 \rightarrow 2$ parton splitting formulations used in the PYTHIA [4, 5, 6] and HERWIG generator families [7, 8], are themselves problematic due to the need for momentum reshuffling to preserve Lorentz invariance in PS evolution: their off-shell intermediate parton representations may not have physically reasonable four-momenta, nor even be represented in a well-defined reference frame. Practically, even if physical information could in principle be obtained for every parton in a given MC generator’s event record, it would be extremely inconvenient to require separate algorithms for each generator’s event records.

In this paper we propose and characterise an alternative truth-jet labelling method, based on standard jet clustering algorithms and measures, modified to only permit clusterings compatible with $1 \rightarrow 2$ QCD and QED processes. This has been implemented in the FastJet framework for three standard jet measures, and we present studies of the performance, robustness and portability of the resulting labels across physics processes, perturbative orders, PS event generators, distance measures, and soft physics effects.

The primary motivation for this work is to provide an operational definition without the practical problems of ill-defined clustering inputs and generator-incompatibility which plague existing truth labelling schemes. However, we note the close relation of this scheme to prior work on infrared safety in partonic jet definition [9] and discuss possibilities for extension of

this scheme both for improved perturbative safety and for use in tagging beyond the regime of Sudakov emission kinematics.

1 QCD-aware parton clustering

The “QCD-aware” clustering algorithm which we will characterise in this paper is directly intended to address the limitations enumerated in the previous section. Our priority is to obtain a robust truth-jet labelling scheme usable with all event generator codes, and based on physically well-defined partons, and not at present the issues of QCD singularities focused on by the related flavour- k_T algorithm [9].

1.1 Jet clustering algorithms

QCD-aware clustering is, like flavour- k_T , a modification of the well-established k_T^{2n} family of agglomerative jet clusterings, developed as an infrared & collinear safe alternative to cone-based jet finding [10]. These operate by clustering an initial population of would-be jet constituents (particles, or experimental objects such as calorimeter cell clusters), known as *pseudojets*, into final jets by repeated $2 \rightarrow 1$ combinations of pseudojets. At each iteration of the algorithm, the pair of pseudojets to be combined is that which minimises a distance measure containing energy and angular terms. The distance measure for the k_T^{2n} family is

$$d_{ij}^{(n)} = \min \left(k_{T,i}^{2n}, k_{T,j}^{2n} \right) \Delta R_{ij}^2 / R^2 \quad (1)$$

where i and j are the pseudojet indices, ΔR_{ij} is the beamline-boost-invariant distance between them in η - ϕ or y - ϕ space, R is a parameter defining the characteristic radius of the resulting jets, and the choice of n exponent chooses whether the algorithm is “ k_T ” ($n = 1$), “Cambridge-Aachen (C/A)” ($n = 0$), or “anti- k_T ” ($n = -1$)¹. A pseudojet i is considered “final” and removed from the clustering if its nearest distance to another pseudojet is greater than $k_{T,i}^{2n}$, the so-called beam distance. Clustering stops when no pseudojets remain.

The formal origins of this family of clustering distances lie in the form of the measure, which for the original k_T measure is proportional to both the smallest transverse momentum and to ΔR . This focus on the low- k_T and small emission angle regions ensures resummation of both the collinear and soft divergences in the QCD gluon emission splitting function, and k_T clustering is often referred to as an inversion of the QCD emission sequence of a parton shower or resummation². The later C/A and anti- k_T algorithms only address the collinear divergence,

¹Other, potentially non-integer, values could also be used but have received little attention since the sign of n is more important than its absolute value.

²The aim of the flavour- k_T algorithm was to make this inverse relationship more precise, by using a distinct distance measure for the purely collinear divergence of the $g \rightarrow q\bar{q}$ parton splitting.

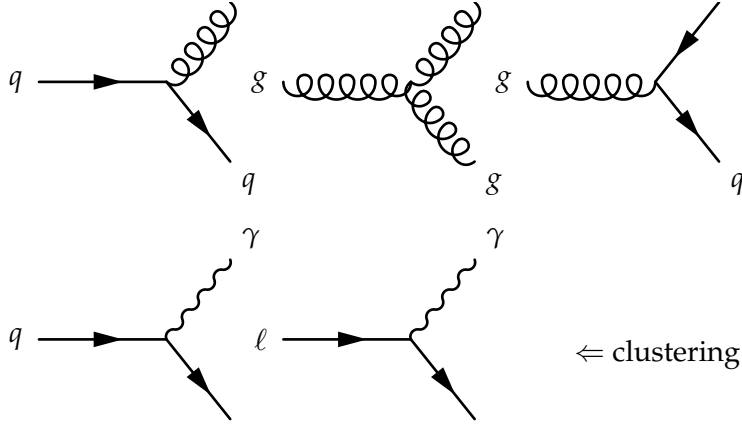


Figure 1: Feynman rule vertices used for QCD (and QED) aware jet clustering.

but due to its production of circular jets the latter has become the standard jet type used at the LHC. The FastJet [11] package contains several important optimisations for the k_T^{2n} family, making use of geometric properties of the clustering measures to ameliorate the naïve cubic dependence on the number of initial pseudojets.

1.2 Flavour-aware clustering

The relationship between jet clustering and dominant QCD emission kinematics is central to the QCD-aware approach to truth jet labelling. The “first” partons connected to a MC generator signal process suffer from an unphysical distinction between matrix element and shower emissions, as well as uncertainty over the physicality of their momenta, but inversion of the emission sequence starting from more physical final partons should in principle be well-behaved.

We hence propose a minor modification to the above family of clustering algorithms, in which the measure is adapted to ensure that only clusterings compatible with the 3-point Feynman rules of QCD and QED will be granted a finite distance. The vertices corresponding to these Feynman rules are shown in Figure 1. Note that charged leptons and photons are also included. The “QCD-aware” distance measure is hence

$$D_{ij}^{(n)} = \begin{cases} d_{ij}^{(n)} & \text{if flavours QCD/QED compatible,} \\ \infty & \text{otherwise.} \end{cases} \quad (2)$$

As the effect is to veto flavour-incompatible clusterings which *would* take place in a standard flavour-blind jet algorithm, all the FastJet performance optimisations for the $k_T^{(n)}$ family could also apply to the QCD-aware variants of those algorithms.

For this to work, each pseudojet must carry an extra fundamental particle flavour label in

addition to the usual kinematic information, and this label must be set on the resulting pseudojet from each $2 \rightarrow 1$ merging, as required by consistency with the corresponding Feynman rule. This measure modification and relabelling algorithm are implemented in the `QCDAware FastJet` plugin class.

It is important to note some simplifications in our scheme. First, we have ignored the 4-gluon vertex since it cannot be mapped to a $2 \rightarrow 1$ clustering and has a small splitting function. Secondly, we do not permit ambiguity: a $q\bar{q}$ clustering could in principle resolve to either a gluon (as implemented) or a photon³. One could consider both “histories” to be valid, assign weights according to computed relative probabilities, and eventually marginalise labelling results across the weighted ensemble of potential histories: this would be an approach along the lines of the shower deconstruction method [12]. Instead, for definiteness and computational tractability, we ignore the QED solution in favour of the much stronger strong coupling. Finally, we use a bare k_T measure where the flavours are consistent, with no weighting for distinct splitting kinematics cf. flavour- k_T , nor for the relative strengths of (running) α_S and α_{QED} or the relevant charges of the participating particles. This last set of points is certainly worthy of consideration, but as we shall see even the bare algorithm exhibits interesting and useful features.

Finally we highlight a somewhat obvious property of flavour-aware clustering which is useful to bear in mind: that the majority of emissions consist of emission of the gauge boson, i.e. the gluon or photon for strong and EM radiation respectively, and that this produces no flavour change. We would expect that it would be relatively hard for a quark jet to lose its quark label (this would require an accidental clustering with an antiquark of the same flavour), while a true gluon jet can be mislabelled as a quark jet by the accidental presence of a single quark within its capture radius. (The same applies to should-be isolated photons contaminated by the proximity of a quark or charged lepton.) We will consider this effect later, particularly when studying systematic variations on MC generator configurations.

2 Selection of clustering inputs

Before the “QCD-aware” clustering rules can be used to generate labelling parton-jets, we must identify the partons, photons, and leptons to be clustered.

Only the final quarks and gluons — those immediately before hadronisation — are used as inputs to the clustering. This avoids double-counting, since the partons in question are guaranteed not to have undergone any further splittings or radiation, and we have verified that the three main families of parton shower MC generators record the momenta of these partons in the lab frame⁴. The representation of final partons is not uniform between generators, so

³For now we also do not consider the $\ell^+\ell^- \rightarrow \gamma$ inverted photon conversion as an allowed clustering.

⁴This is not a standard imposed by the HepMC [13] event record standard, but perhaps it should be.

we apply a two-step heuristic to identify them: first we accept a parton if it is incoming to a vertex with `status/id = 5`, the standard code for a hadronisation vertex; and secondly, if the first condition is not met, the particle is accepted if it has no children which are also partons. The first condition is preferable, but hadronisation vertex labelling is currently only implemented in Sherpa, hence the second heuristic is required to identify final partons in Herwig++ and Pythia 8.

Photons, electrons, muons, and hadronically-decaying taus that have no hadronic ancestors (“prompt”) are included in the clustering inputs. The “prompt” restriction is because the four-momentum associated with non-prompt photons and leptons is already included in the momenta of the final partons whose descendent hadrons decay to them. The restriction to hadronic taus is for alignment with experimental procedure: taus that decay to leptons are generally reconstructed by experiments as charged leptons and missing energy rather than as jets, with such charged leptons from prompt taus being themselves classified as prompt.

An implementation of this input-selection algorithm is available in the `FinalPartons` and `TauFinder` projections in Rivet [14] from version 2.2.1 onwards.

3 Associating labels to jets

After applying the QCD-aware clustering to the partonic (and prompt lepton and photon) inputs discussed above, and normal flavour-blind clustering to the final state truth particles, we have two distinct jet collections: flavoured partonic label-jets, and standard particle jets. We aim to label the latter using the former.

Arguably the simplest labelling algorithm is to assign each particle jet the label of the closest parton jet, i.e. that which minimises $\Delta R_{\text{jet-label}}$. This has the drawback, however, that distinct particle jets can share the same closest parton jet: should the particle jets share the same label, or should some additional matching criterion be introduced to assign the parton jet to just one particle jet, e.g. the nearer of the two?

In this study we have hence used the ghost association [15] method to non-invasively cluster the parton jets into the particle jets, guaranteeing that no parton label will be associated to multiple particle jets⁵.

A second ambiguity now arises, because more than one parton jet can be ghost-associated to a given particle jet. Since the QCD-aware clustering forbids combination of some parton flavours, having multiple unclustered partons within a particle jet’s clustering radius is a fairly frequent occurrence – moreso than the many-particle-to-one-parton ambiguity that ghost association resolves. Hence a disambiguation measure is required among the associated parton jets, and for simplicity we have chosen the label which minimises $\Delta R_{\text{jet-label}}$, within an inner core of the

⁵Note that this is for the purposes of definiteness more than absolute physical correctness: in such ambiguous circumstances there is no guarantee that ghost association has picked the physically “correct” assignment, or that such a thing even exists.

jet radius: if all $\Delta R > 0.2$, the jet remains unlabelled. This restriction to $\Delta R < 0.2$ was added to remove long, low rate tails observed in initial runs of the algorithm. This may certainly be improved, and we suggest either a combined ΔR and p_T matching measure (although this is a little like adding apples and oranges), to favour high- p_T or well-matched p_T labels within the jet cone, and/or to assign weights rather than absolute labels – but we do not consider such extensions in this paper.

4 Performance of QCD-aware labelling

In this section we will make performance comparisons of the above-described labelling algorithm for two hard processes, dijet and γ -jet, with various parton shower event generators, and with several systematic variations to both the labelling scheme and to the simulation:

Shower generators: Pythia 8.201, Herwig++ 2.7.1, Sherpa 2.1.1

Clustering variants: max- p_T (no clustering) / k_T QCD-aware / anti- k_T QCD-aware

Simulation variants: normal / without MPI / raised shower cutoff / ME max multiplicity

Association variants: all labels / reclustered labels

A minimum p_T requirement of 25 GeV has been imposed on the particle jets in these studies, and a $p_T > 5$ GeV requirement on the partonic label jets. Both types of jets were clustered with an R parameter of 0.4. All jet clustering was restricted to within $|\eta| < 2.5$.

For comparison to the QCD-aware approach, we will present a “maximum p_T ” partonic jet labelling scheme, where the label assigned to a final-state truth jet is the flavour of the highest- p_T parton within its radius. This label is discovered by looping over *all* partons, including those in the hard process final state (typically in the partonic centre-of-mass frame of the matrix element calculation), through all the intermediate stages of the parton shower and MPI, down to the final partons described in Section 2 on page 5. Since the highest- p_T parton is used, this tends to be from the hard process or shortly after, before it has radiated significant virtuality via shower branchings. The measures that we use for labelling kinematic performance would be biased in this scheme, hence we will only show it in direct comparisons either of label assignments or in ratios of flavour label rates.

4.1 MC generator families

A key motivation for the QCD-aware approach to partonic truth-jet labelling is for the method to be portable between different MC generators. Each plot in most of the following studies is

hence shown with three MC lines, for the three major parton shower MC generator families; the exact versions are given above.

In principle, the QCD-aware method should be robust enough for use both with fixed-order codes (producing a few-body partonic final state) and parton shower codes in which the final-state partonic multiplicity is much higher. Substantial differences between the Herwig and Pythia generator families have been seen in q/g rate prediction studies using the max- p_T labelling scheme [16, 17], so some level of variation is to be expected between generator shower formalisms, but we expect broad qualitative agreement of labelling both between generators and with the expectations for each hard process type.

In particular we are interested to see how the Sherpa generator compares to the Herwig and Pythia families, since it has not previously been possible to include Sherpa in partonic labelling studies.

In all the plots that follow in this section, all three generators have been configured to use only lowest-order $2 \rightarrow 2$ hard scattering matrix elements, so that any differences are due to MC family differences in parton shower algorithms, and matrix element scale choices.

More specific modelling variations within generator families are considered in Sections 4.4 and 4.5, using only Pythia and only Sherpa respectively.

4.2 Performance of default QCD-aware labelling

In Figures 2 and 3 we show the p_T resolution, $\Delta p_T/p_T = (p_T^{\text{jet}} - p_T^{\text{label}}) / p_T^{\text{jet}}$ and ΔR measure between the particle jets and their assigned labels in the inclusive-QCD-jet process. The light parton measures are shown for the photon+jet hard process type in Figure 4, the less interesting heavy label performance being relegated to Appendix A. A k_T measure has been used in the construction of the QCD-aware labelling jets, but the particle jets are anti- k_T as is standard for the LHC experiments; the effect of this mismatch will be investigated in Section 4.3 on page 13. The effect of ME scale dependence on the plot normalisation has been largely eliminated by rescaling all histograms to correspond to the Pythia 8 cross-section calculation.

The main point of note in these plots is general consistency between generators, and good-quality kinematic matching of the labels to the particle jets. The consistency is not perfect – for example Pythia events feature significantly more bottom-labelled jets than either of the other generators in the jets process, and Herwig++ produces many more gluon-labelled jets in the $\gamma + \text{jet}$ event type – but otherwise these resolutions are very compatible both with each other and with the expectations of approximate parton–jet duality. Where shape differences are seen, e.g. the Herwig++ high tail for light-quark-labelled $\Delta p_T/p_T$ in jet events, they are significantly suppressed relative to the peak of the distribution; addition of a p_T resolution window cut to the labelling algorithm could remove the few anomalous labels assigned from long tails such as this.

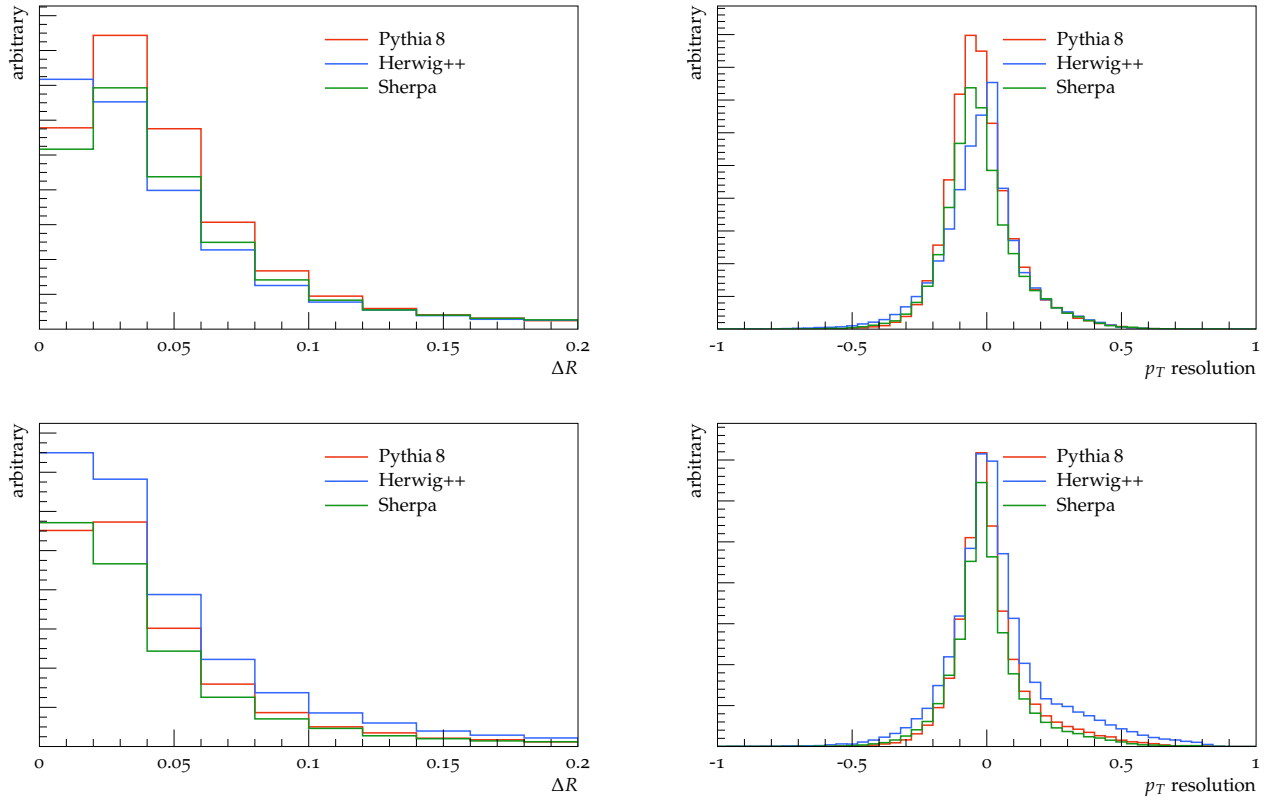


Figure 2: Light tagging performance/comparisons: inclusive jet events, with gluon-labelled jets on the top row and light-quark-labelled jets on the bottom row. Particle jets clustered using the anti- k_T algorithm, labelling parton jets with the k_T algorithm.

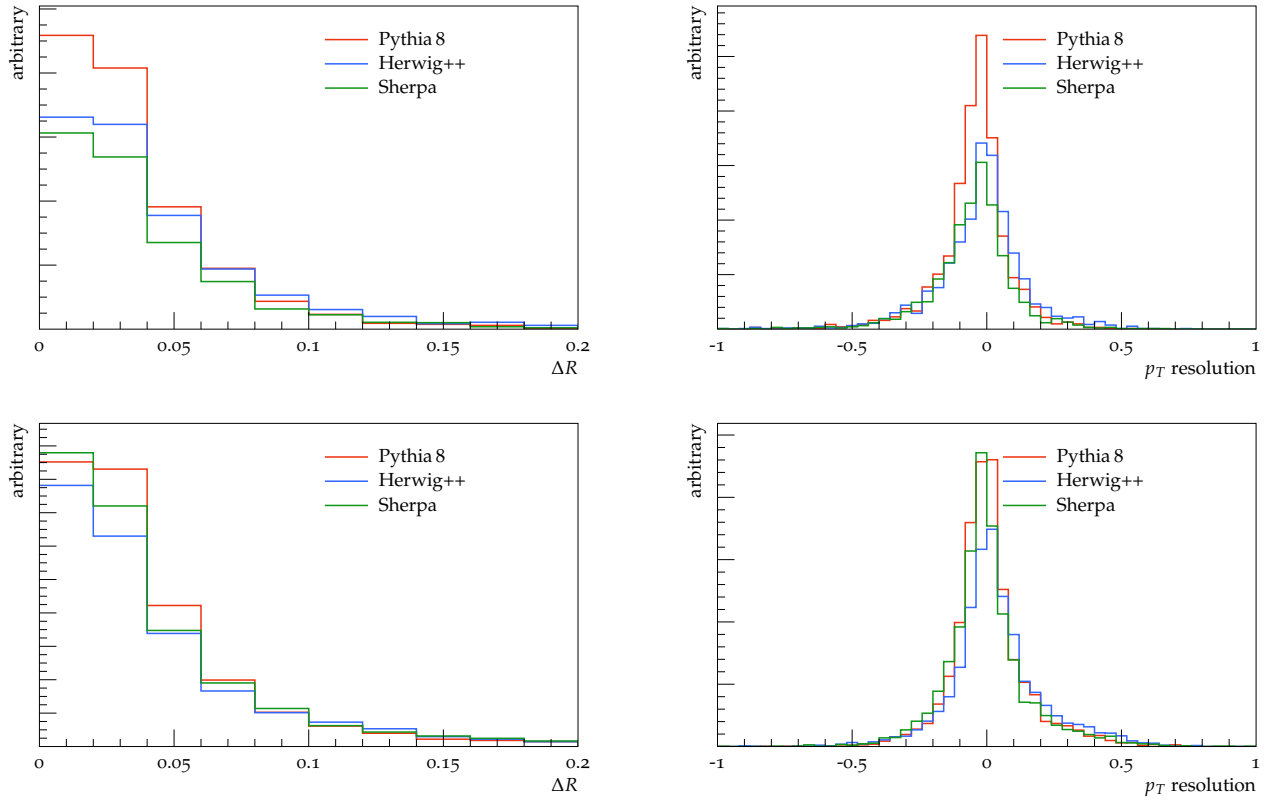


Figure 3: Heavy tagging performance/comparisons: inclusive jet events, with bottom-labelled jets on the top row and charm-labelled jets on the bottom row. Particle jets clustered using the anti- k_T algorithm, labelling parton jets with the k_T algorithm.

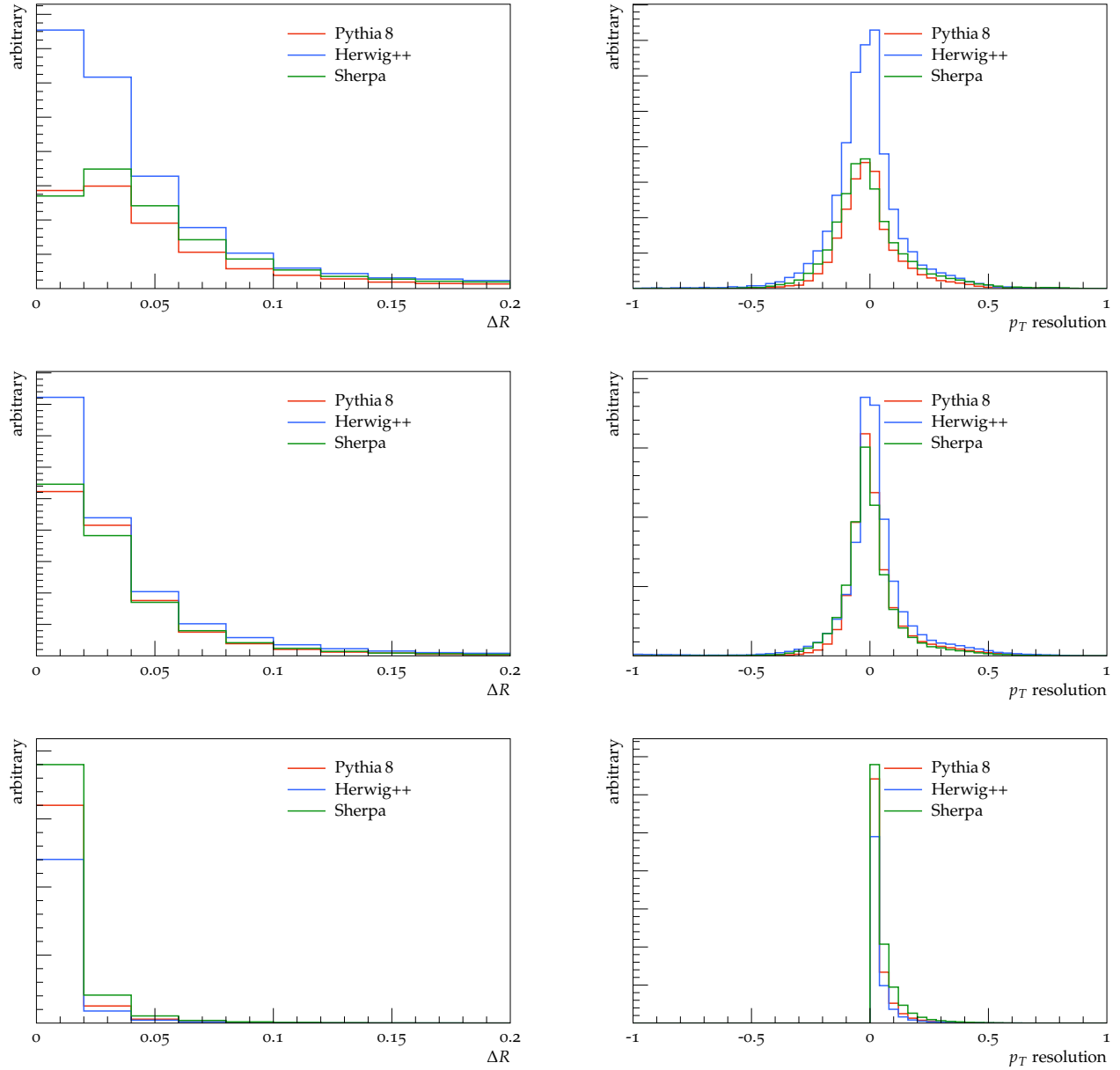


Figure 4: Light tagging performance/comparisons: γ + jet events, with gluon-labelled jets on the top row, light-quark-labelled jets in the middle row, and isolated prompt photons on the bottom row. Particle jets clustered using the anti- k_T algorithm, labelling parton jets with the k_T algorithm. The one-sided p_T resolution distribution for the photon-labelled jet is by construction as described in the text.

Scheme	Generator	Jets	$\gamma + \text{jet}$	
		q/g	γ/g	q/g
Max- p_T	Pythia 8	0.38	17.2	10.5
	Herwig++	0.33	7.7	4.8
	Sherpa	0.55	21.0	9.6
k_T	Pythia 8	0.80	10.4	8.2
	Herwig++	1.17	3.6	4.6
	Sherpa	0.85	10.5	7.5
anti- k_T	Pythia 8	0.79	10.2	8.3
	Herwig++	1.74	3.2	4.5
	Sherpa	0.86	10.2	7.5
Reclustered	Pythia 8	0.77	10.1	8.0
	Herwig++	1.36	3.5	4.8
	Sherpa	0.83	10.1	7.3

Table 1: Jet label ratios for the combined sample of leading and subleading jets constructed in inclusive jet and $\gamma + \text{jet}$ simulated events, for various MC generators.

The one-sided Δp_T distribution for the $\gamma + \text{jet}$ samples is deserving of explanation. This feature is by construction: to be labelled as a photon, the labelling “parton” is the exact same final-state photon as will enter the particle-jet finding, because there is no parton that a photon can cluster with, without losing its flavour. Hence the total jet p_T must be at least the same as the labelling photon: momentum can only be added, not subtracted, within the jet cone. By contrast, for quark or gluon jets there are non-perturbative processes such as hadronisation and colour-reconnection which can reduce the particle-jet energy below that of their labelling parton. It is likely that an asymmetry of similar size is convolved into the $\Delta p_T / p_T$ distributions for quark and gluon jets, but that their overall greater width from non-perturbative modelling dominates the roughly symmetric peak shape.

4.2.1 Flavour label ratios

The other feature of these plots immediately worth commenting on is how the total number of jets labelled as gluon or quark in these two samples compare to the cross-sections of the fixed-order subprocess matrix elements. We compute these ratios from the integral of each distribution for the two leading jets only, to ensure final-state quantities comparable to the 2-particle matrix element final states, and are not biased by the propensities of the generators to produce different numbers of above-threshold jets. The summary ratios are presented in Table 1, and we now discuss them for the two process types.

Inclusive jet sample: the Pythia 8 leading-order matrix elements had the following cross-sections:

$\sigma(gg \rightarrow gg) = 2.71$ mb, $\sigma(qg \rightarrow qg) = 1.41$ mb, $\sigma(qq \rightarrow qq) = 0.15$ mb, $\sigma(gg \rightarrow q\bar{q}) = 0.07$ mb. Summing these according to their contributions to the rates of final state quark or gluon partons, a fixed-order quark/gluon jet ratio of 0.27 is expected.

Comparing the normalisations of the simulated gluon and quark observables gives QCD-aware k_T quark/gluon labelling ratios of between 0.8–1.2 for the three shower generators, with Herwig++ at 1.17 a clear outlier from the other two generators near 0.8. The equivalent range for the max- p_T labelling scheme is 0.33–0.55. There is hence a substantial difference between the q/g ratios obtained from max- p_T and QCD-aware schemes, the max- p_T scheme giving label rates closer to the fixed-order expectation than QCD-aware – although this should not be overinterpreted as indicting (in)correctness of either scheme.

The inverted q/g ratio from Herwig++ is due to an excess of quarks, clearly visible in the light-quark plots of Figure 2 on page 9. Requiring a jet-label p_T match by cuts on the tails of p_T resolution brings the Herwig++ q/g ratio to 1.0 – closer to the others, but still not good agreement.

γ + **jet sample:** applying the same methodology as for the inclusive jet ratios, the two tree-level subprocess cross-sections are $\sigma(qg \rightarrow q\gamma) = 650$ nb and $\sigma(q\bar{q} \rightarrow g\gamma) = 53$ nb, corresponding to expected fixed-order photon/gluon and quark/gluon ratios of 13.2 and 12.2.

The fully showered QCD-aware k_T ratios are between 3.6–10.4 and 4.6–8.2 respectively, and the max- p_T equivalents are 7.7–21.0 and 4.8–10.5. In both schemes, there is agreement between the rates for Pythia8 and Sherpa which are at the high ends of the ratio ranges for both processes, but Herwig++ is highly discrepant. The much lower γ/g and q/g rates for Herwig++ appear to be driven by its very high gluon rate, clearly visible in Figure 4 on page 11; there is this time no obvious matching cut on ΔR or p_T resolution which could address this issue.

We stress again that these predictions are subject to significant resummation corrections and hence do not identify the “right answer”. The broad expectations from fixed order subprocess cross-sections are met by Sherpa and Pythia8, but Herwig++ significantly deviates from the other generators by producing unusually many quark jets in jet events, and gluon jets in γ + jet events. We will return to these features later.

4.3 Dependence on clustering distance measure

In our introduction of the QCD-aware method, we motivated partonic clusterings by analogy to a “rewinding” of QCD evolution through gluon radiation (and the analogous evolution for photon emission). This was also the historical motivation for the flavour-blind “bland” k_T clustering, but

		k_t label					
		none	g	q	c	b	γ
anti- k_t label	none	0.8	0.1	-	-	-	-
	g	0.3	52.5	2.5	0.1	-	-
	q	0.1	2.1	33.7	-	-	-
	c	-	-	-	5.0	-	-
	b	-	-	-	-	2.5	-
	γ	-	-	-	-	-	-

		k_t -reclustered label					
		none	g	q	c	b	γ
k_t label	none	-	0.9	0.3	-	-	-
	g	-	53.0	1.6	-	-	-
	q	-	2.5	33.8	-	-	-
	c	-	0.1	-	5.0	-	-
	b	-	-	-	-	2.5	-
	γ	-	-	-	-	-	-

		max- p_T label					
		none	g	q	c	b	γ
k_t label	none	-	1.1	0.1	-	-	-
	g	-	53.5	1.1	-	-	-
	q	-	15.7	20.5	-	-	-
	c	-	1.5	-	3.6	-	-
	b	-	0.4	-	-	2.1	-
	γ	-	-	-	-	-	-

Table 2: Correlation matrices for pairs of labelling schemes in Pythia inclusive jet events. Each entry shows the fraction of all jets (in percent) given a pair of labels by the schemes listed on the vertical and horizontal axes. q here denotes a light-quark label. Fractions less than 0.1% are replaced with a dash.

it has since proven useful to use alternative measures, most notably the anti- k_T distance which has no clear link to resummation. We here entertain the possibility that the anti- k_T distance measure may prove to have useful properties despite its relative lack of *a priori* motivation.

To reduce the potential for kinematic mismatch of k_T and anti- k_T jet shapes, we also consider a k_T -based QCD-aware reclustering of final partons matched to anti- k_T particle jets. In this approach, final partons are first ghost-associated [15] as part of the construction of anti- k_T particle jets, then for each particle jet the collection of associated final partons is clustered using the QCD-aware k_T measure (“ k_T -reclustered”). The anti- k_T particle jet then inherits the label of the k_T final parton jet with the smallest ΔR separation to its axis.

In Figure 5 the $\Delta p_T/p_T$ performance measure is again shown for the three shower MC generators, for gluon- and quark-labelled jets, respectively. The ΔR performance comparisons are shown in Figure 10 in the appendix. Figure 6 shows a direct comparison of these spectra across labelling schemes for Pythia inclusive jet events. Perhaps surprisingly, the differences in shape are small, even though anti- k_T is expected to have a virtually meaningless cluster sequence. There are two explanations for this: first, the flavour combination rules mean that there is much less difference in the clustering sequence than would be the case in a normal flavour-blind k_T vs. anti- k_T clustering comparison; and second, the resulting labels often depend not on the detailed order of clusterings but on *whether* an unpaired (anti)quark ever gets clustered into

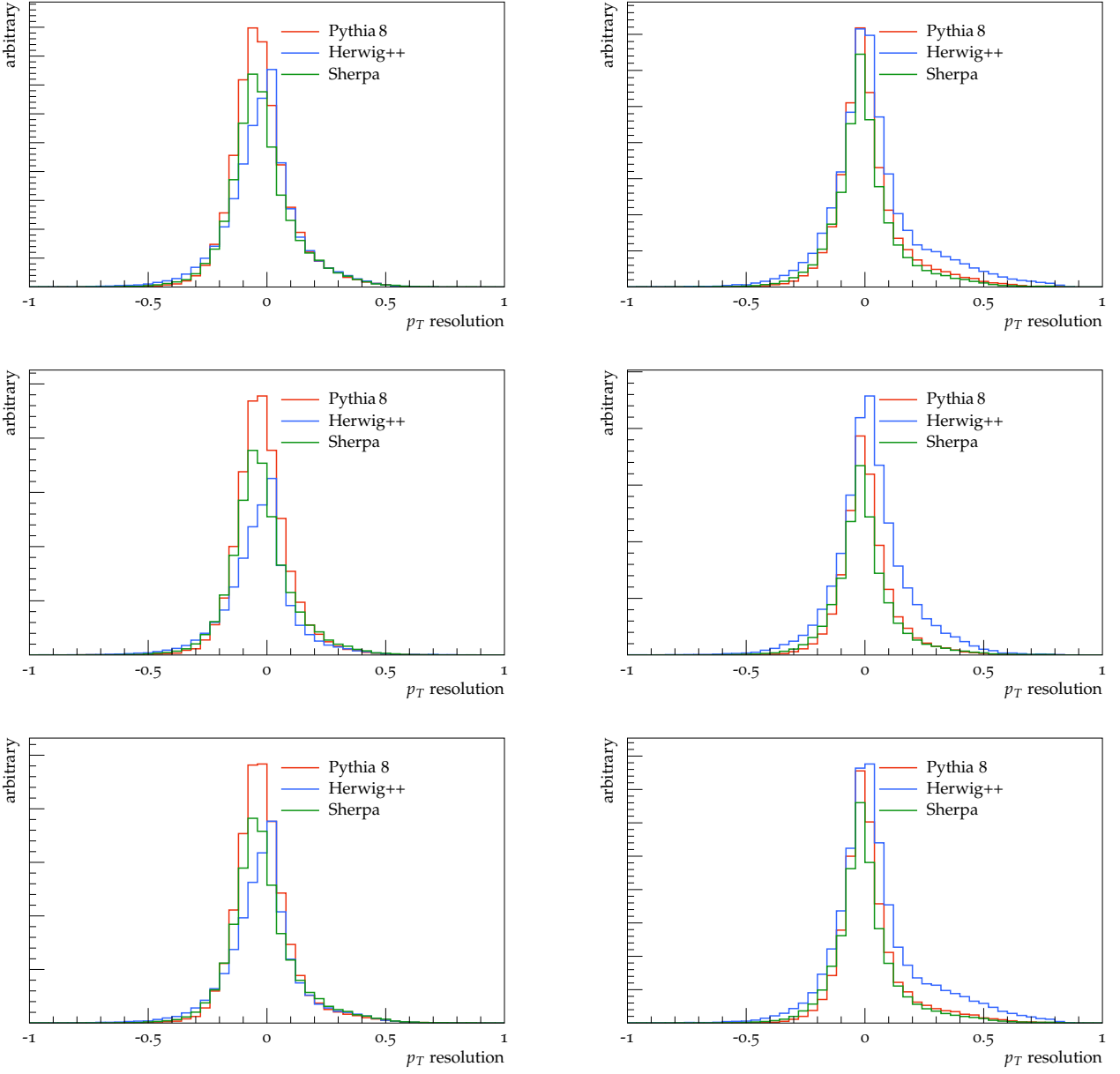


Figure 5: $\Delta p_T/p_T$ performance comparisons for gluon- (left) and light quark-labelled jets (right) in inclusive jet events, showing k_T labeled jets on the top row, anti- k_T in the middle, and k_T -reclustered on the bottom.

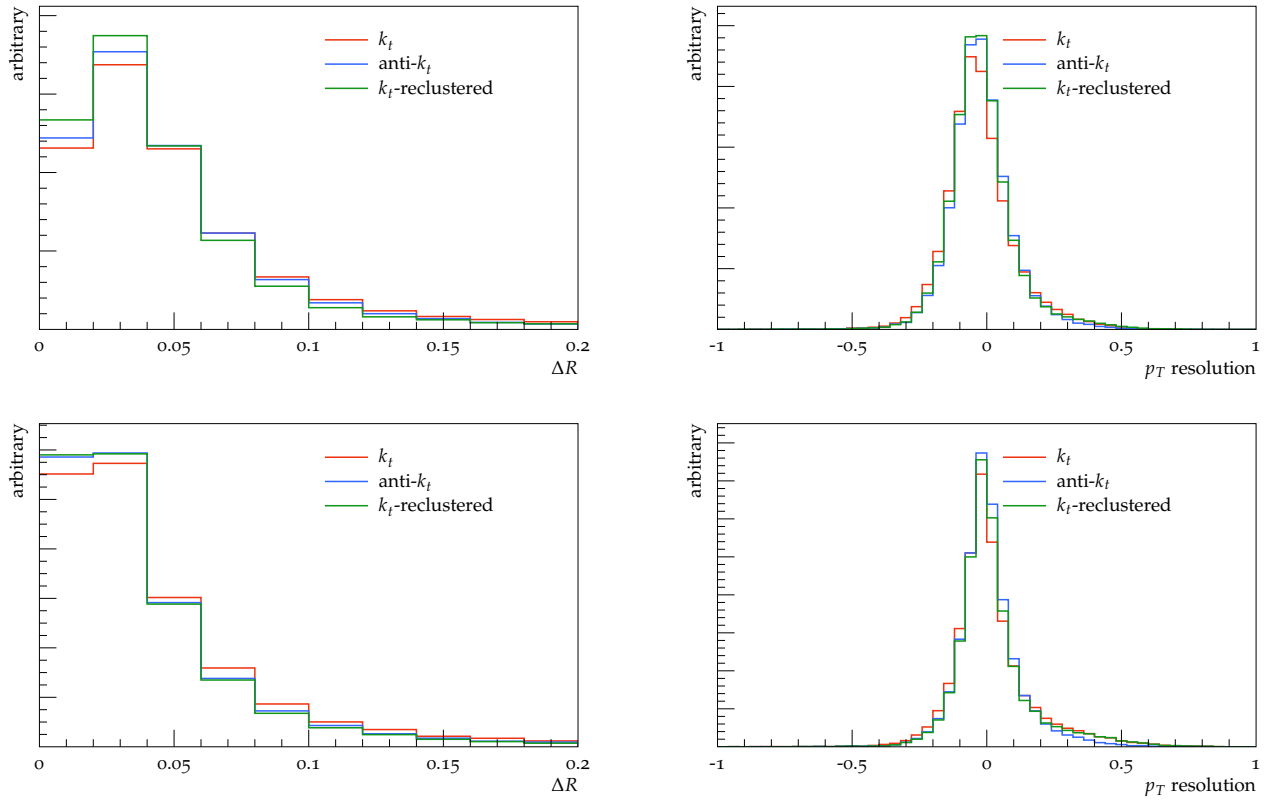


Figure 6: ΔR (left) and $\Delta p_T / p_T$ (right) clustering performance comparisons for gluon (top) and light (bottom) labelled jets in Pythia inclusive jet events.

		max- p_T label					
		none	g	q	c	b	γ
k_t label	none	-	0.2	0.3	-	-	0.6
	g	-	5.6	2.7	0.2	-	2.8
	q	-	4.3	25.6	0.2	-	14.7
	c	-	0.2	-	6.1	-	0.3
	b	-	-	-	-	0.9	-
	γ	-	-	-	-	-	34.8

		max- p_T label					
		none	g	q	c	b	γ
k_t label	none	-	-	0.2	-	-	0.9
	g	-	3.1	1.8	0.2	-	0.4
	q	-	0.9	27.5	-	-	3.4
	c	-	-	-	6.4	-	0.2
	b	-	-	-	-	0.9	-
	γ	-	-	-	-	-	53.8

Table 3: Correlation matrices for pairs of labelling schemes in Herwig++ γ + jet events with MPI on (left) and MPI off (right). Each entry shows the fraction of all jets (in percent) given a pair of labels by the schemes listed on the vertical and horizontal axes. q here denotes a light-quark label. Fractions less than 0.1% are replaced with a dash.

an otherwise gluon-flavoured parton pseudojet. Clustering of gluons or photons on to a quark or lepton-flavoured pseudojet changes only kinematics, not the label, and the change to the kinematics is invariant of the order of the boson clustering – the effect of measure is hence largely relegated to clusterings near the jet radius and those which occur during the differing periods during which the pseudojet kinematics are stabilising.

How the labels of individual particle jets differ between schemes is also of interest. For instance, the k_T scheme may assign a jet a gluon label while the anti- k_T scheme may label it as a quark. This is summarised in the label correlation matrices in Table 2. The anti- k_T and k_T -reclustered schemes are in the top row, while the bottom-left matrix compares QCD-aware k_T with the max- p_T scheme, in which a particle jet inherits the label of the highest- p_T ghost-associated parton from *any* step of the QCD shower evolution. Labelling algorithms similar to the max- p_T scheme have been used in performance studies at ATLAS [18].

Table 3 gives some indication of the origin of the difference between max- p_T and QCD-aware labelling for Herwig++ γ + jet events: there is a very significant off-diagonal contribution in the q - γ cell, i.e. jets which are identified as photons in the max- p_T scheme, but as quarks in the QCD-aware scheme. This implies that low-momentum quarks in the vicinity of the hard photon are “capturing” that hard object and stealing its photon label. The unanswered question is why only Herwig++ and not Pythia or Sherpa have such a significant population of low-momentum quark “pollution”. This deserves further investigation which would not be appropriate here, both investigating the effects of various Herwig++ model features and a more nuanced treatment of q - γ clustering in the QCD-aware algorithm.

In the absence of strong empirical motivations to choose the anti- k_T or k_T -reclustered labelling schemes, the k_T measure remains the most obvious choice due to its theoretical links to QCD (and QED) emission kinematics in the Sudakov regime, and because where scheme-dependent anomalies are seen, they appear to be more prevalent in the anti- k_T and reclustered- k_T schemes.

4.4 Dependence on parton shower IR-cutoff and multi-parton interactions

In this section we consider two possible systematic effects in the configuration of the MC generator supplying events for jet finding and labelling: the choice of parton shower cutoff scale, and the impact of multi-parton interactions. In both cases the process of gluon splitting to quarks is the most dangerous to the stability of the jet labelling, since a wide angle soft splitting may not be clustered back together (without a distance modification *à la* flavour- k_T) in this early clustering phase, leaving two lone quark labels free to contaminate other gluon pseudojets.

4.4.1 Parton shower IR-cutoff

In principle, the QCD-aware labelling technique can be passed a partonic final state at any stage of its evolution and the results should remain largely invariant, since the low- p_T evolution should be safely reversed in the clustering. To test this hypothesis we have run Pythia 8 with both a normal ($\mathcal{O}(1 \text{ GeV})$) parton shower cutoff, and one in which that cutoff has been greatly raised to the jet p_T threshold of 30 GeV. The effect of this is seen in Figure 7, and acts both as a very conservative estimate to the algorithm’s sensitivity to the IR region of shower evolution (where different MC generators may use different cutoff tunes) and an indication of the applicability of the algorithm to appropriately defined fixed-order simulations.

From these plots, comparing the blue raised-cutoff line to the red Pythia 8 default configuration, it can be seen that the low- p_T splittings in the default configuration increase the rate of light-quark jet labels, while having little impact on the gluon-label rate. As well as in the overall normalisations, this effect can particularly be seen in the high “shoulder” in the bottom-right quark-label p_T -resolution observable, which is most prominent for the red default setup. This suggests that the relative ease of q/g contamination leads to “wrong” light-quark labels being derived from gluon splittings to light quarks in the high multiplicity of low- p_T shower branchings, and hints that an improved matching requirement might prefer to label with the highest- p_T label jet close to the particle jet axis in order to reduce this “shoulder” of mismatched too-low- p_T labels.

4.4.2 Multi-parton interactions (MPI)

Multi-parton scattering poses a potentially lethal threat to an algorithm starting from final state partons, because of the intrinsic assumption that at least a k_T -based clustering will be able to reverse the order of QCD splittings. Typically we are only interested (as far as possible) in the hardest partonic interaction, but MPI overlays the partonic final state of that interaction with those from secondary partonic scatters. As a result of this incoherent overlay of distinct partonic final states, the geometrically optimal partonic clusterings may be between partons evolved from different hard processes, which (at least in model terms) are unrelated. This is expected to

Scheme	Generator	Jets	$\gamma + \text{jet}$	
		q/g	γ/g	q/g
Max- p_T	Pythia 8	0.39	15.4	9.5
	Herwig++	0.33	18.3	11.4
	Sherpa	0.57	13.4	7.0
k_T	Pythia 8	0.65	11.8	7.6
	Herwig++	0.68	11.2	8.0
	Sherpa	0.73	13.0	7.0
anti- k_T	Pythia 8	0.65	11.7	7.6
	Herwig++	0.93	11.0	8.1
	Sherpa	0.74	12.9	7.0
Reclustered	Pythia 8	0.64	11.5	7.5
	Herwig++	0.80	11.0	8.2
	Sherpa	0.73	12.7	6.9

Table 4: Jet label ratios for the combined sample of leading and subleading jets constructed in inclusive jet and $\gamma + \text{jet}$ simulated events, for MC generators with MPI modelling disabled.

be particularly problematic for MPI *quarks*, since unlike gluons (or photons) they can lead to a reassignment of “true” gluon jet flavour labels.

All the performance plots shown so far have had MPI modelling enabled, and in the label ratio discrepancies seen in Section 4.2.1 on page 12 – particularly for Herwig++ with respect to the other generators – there are hints that MPI overlay could be responsible. The $gg \rightarrow gg$ process dominates the low- x MPI processes but shower evolution of the MPI partons would be expected to produce some unpaired gluon splittings with a resulting effect. In Figure 7 on the following page we also compare Pythia 8 with and without MPI modelling enabled, to gauge the magnitude of the effect.

It is clear that the green no-MPI configuration gives substantially better ΔR and p_T agreement between the particle jets and their labels, as well as slightly reducing the overall normalisation – both effects are seen in both the gluon and quark distributions. Resolution improvements were also seen, in the unshown charm and bottom performance measures. This normalisation change, however, does not relate to an increased rate of unlabelled jets, but just the lower total number of particle jets in a no-MPI generator configuration (this was checked separately and is not evident from the displayed plots). While the removal of MPI produces narrower distributions than default in all cases, the largest effect is again seen on the upper side of the light quark p_T -resolution observable, where adding soft MPI emissions enhances the p_T -mismatched “shoulder” to the same extent as soft shower splittings did in the previous section.

In Table 4 we show the same jet label ratios as computed before, but now with MPI disabled

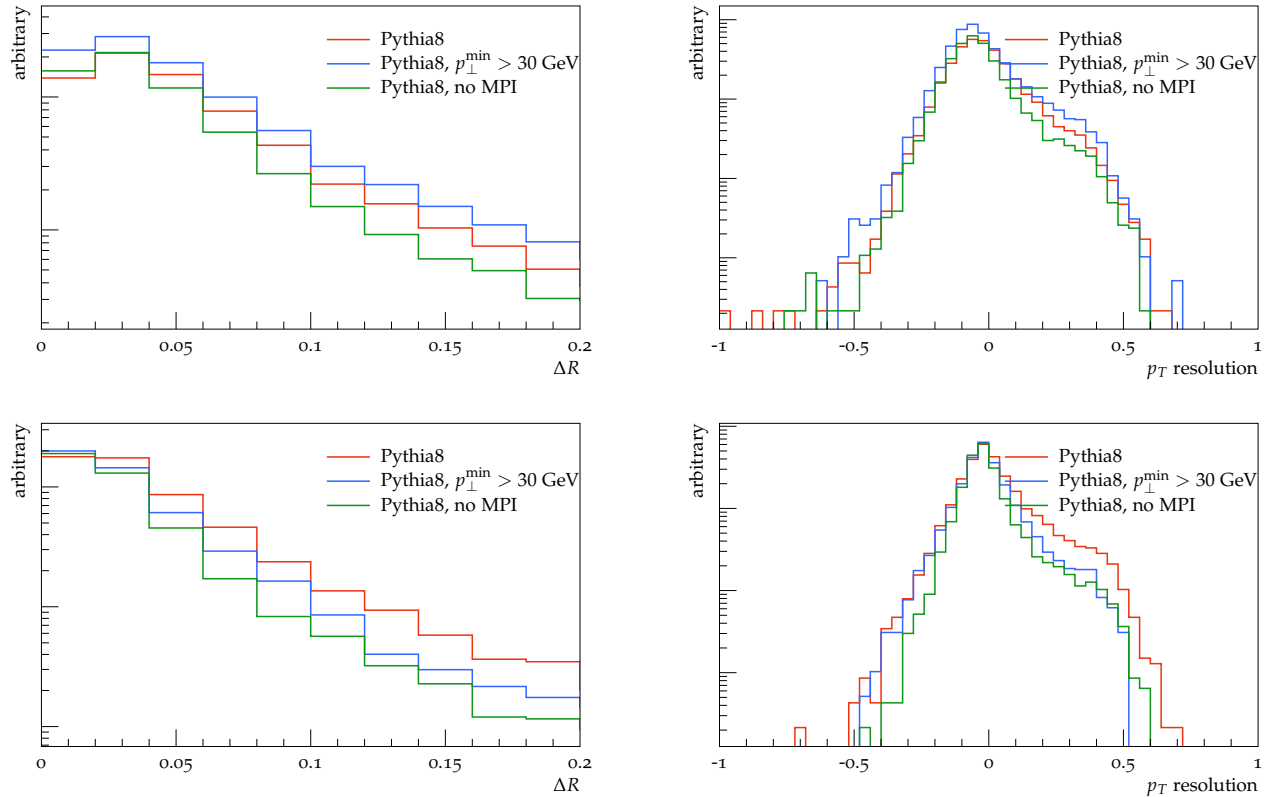


Figure 7: Light tagging dependence on event simulation systematics: inclusive jet events, with gluon-labelled jets on the top row, and light-quark-labelled jets on the bottom.

for all three generators. The difference is striking: the Pythia8 and Sherpa q/g ratios in jet events are little changed, but Herwig++’s “inverted” ratio is now shifted to agree with the others; and in $\gamma + \text{jet}$ events the high Herwig++ gluon rate is now gone, bringing its ratios in line with the other generators (and with very stable, cross-generator values in the QCD-aware scheme). MPI is clearly a very significant problem for post-fragmentation truth-jet labelling algorithms to address.

4.5 Dependence on higher-order ME parton production

In this section we make a final study of the robustness of the QCD-aware labelling scheme, considering variations in the maximum number of matrix element final-state partons for QCD jet events. This study was performed using the Sherpa event generator, configured in three separate runs to use a lowest-order $2 \rightarrow 2$ QCD scattering matrix element as in the previous studies, as well as higher-order tree-level $2 \rightarrow 3$ and $2 \rightarrow 4$ MEs.

The dominance of the lowest-order hard process configuration is illustrated by the stability of the cross-section which rose only by 0.1% from the $2 \rightarrow 2$ value of 3.073 mb with the addition

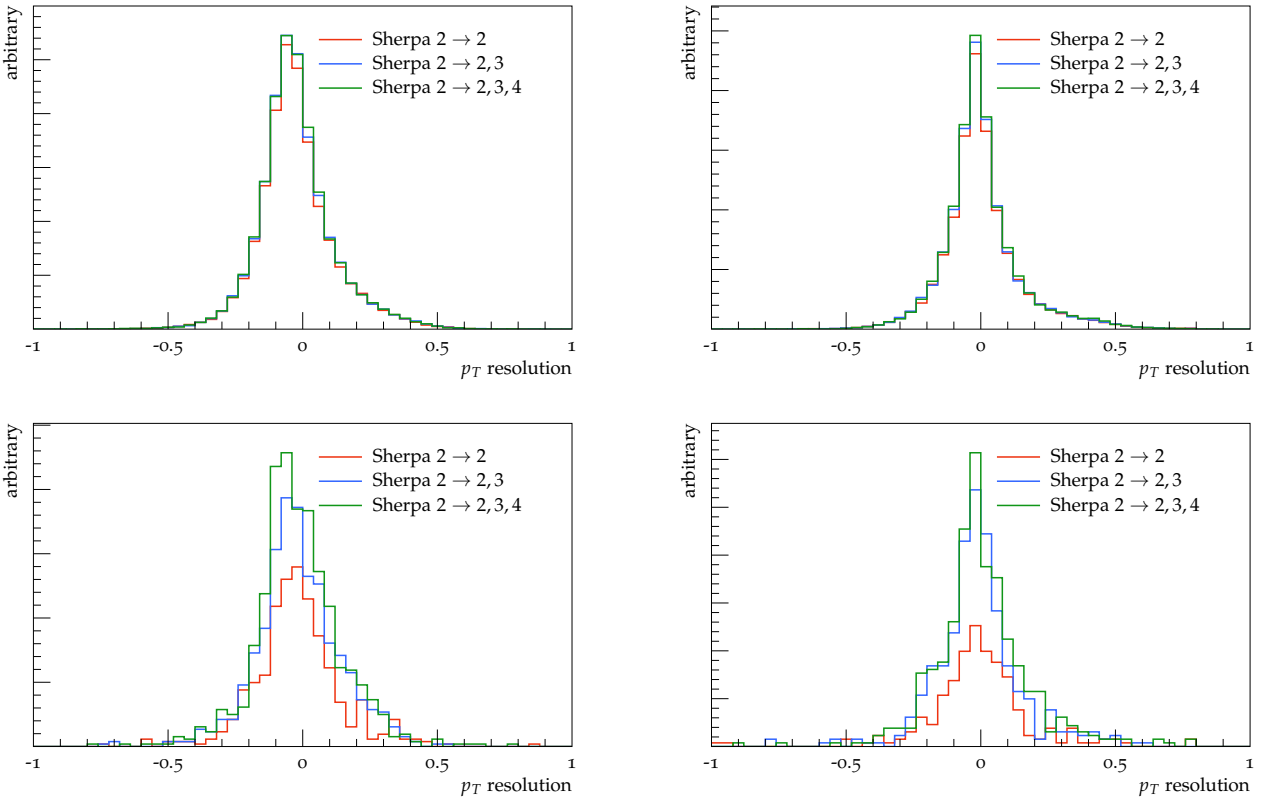


Figure 8: Jet labelling performance dependence on maximum number of ME partons in jet events for gluon- (left) and light quark-labelled jets (right). The top row shows all jets inclusively, the bottom only for the 3rd jet.

ME	$N_{j_3}/N_{j_3}^{2 \rightarrow 2}$	Gluon frac.	Light quark frac.	Light parton frac.	Unlabelled frac.
$2 \rightarrow 2$	1.00	62.7%	27.0%	89.6%	2.3%
$2 \rightarrow 3$	1.59	56.4%	31.4%	88.3%	2.9%
$2 \rightarrow 4$	1.79	58.3%	31.9%	90.2%	2.6%

Table 5: Comparison of 3rd jet rates and flavour label fractions between Sherpa calculation with three different maximal ME final-state multiplicities.

of diagrams with up to two extra final-state partons. The inclusive jet plots in Figure 8 on the previous page show a larger effect, since the total number of jets to pass the 25 GeV analysis p_T cut increased by 4.5% and 5.7% over the 2-parton configuration for the 3- and 4-parton samples respectively. But the stability of the performance measures is still notable.

We see larger differences if we focus on the 3rd-hardest jet in the event, which in the $2 \rightarrow 2$ ME configuration should virtually never directly correspond to an ME parton. The usual labelling performance measures are shown for this in the bottom row of Figure 8 on the preceding page. It is not simple to interpret these plots because the dominant effect is the change in normalisation due to the increased total number of 3rd jets as the matrix elements include more hard corrections: the increases are 59.1% and 79.3% above the $2 \rightarrow 2$ configuration for the 3- and 4-parton MEs respectively. If we instead look at ratios of light quark and gluon labels to the total, shown in Table 5, then stability is again evident: gluon labels account for 58–63% and light quarks for 27–32% of 3rd jets despite the large normalisation changes. The total number of jets labelled as either gluon or light quark remains between 88% and 90% of the total, and the fraction of unlabelled jets is also stable between 2–3%. No asymmetry or change of distribution widths is observed with the changes of ME multiplicity.

We note for clarity that it is not the case that a perfect labelling algorithm would give perfectly stable results in these tests – after all, the physics is being improved with each extra parton, changing the jet kinematics and potentially the flavour balance. But it does suggest both algorithmic robustness and that the light-flavour weighting (if not the kinematics) of the Sherpa parton shower splitting functions is well-matched to the explicit ME calculations.

5 Conclusions and proposals

Just as there is no absolute definition of what constitutes a hadronic jet, there is no absolute way to assign a flavour label to it. But, as for jet finding, there are differences in the algorithms which are used as operational definitions, and not all algorithms are equal.

In this spirit, we have described and characterised the performance of the QCD-aware algorithm for truth jet partonic labelling. This algorithm is based on restricting flavour combinations to those permitted within QCD and QED, and on final state partonic inputs defined in the lab

frame. It offers a theory-motivated labelling approach portable between all the major families of parton shower event generators, and shows fairly low sensitivity to calculation artefacts such as parton evolution cutoffs and ME order. Comparable labelling performance was seen between the generator families, across a range of hard process types with multi-parton interactions (MPI) disabled: the ratios of jet label rates from the three generators were in good agreement with each other, and the dominant labels agreed with the prediction from fixed-order cross-sections. A lack of strong dependence on distance measure was observed, due to the constraining effects of the flavour combination rules. Hence, while “just another algorithm”, we contest that the QCD-aware approach is better theoretically motivated than existing approaches and portable between MC shower generators in the absence of MPI, e.g. in e^+e^- events.

However, the labelling performance *is* affected by MPI, which introduces a “shoulder” structure several times higher than the no-MPI rate into the tail of the labelling jet p_T resolution, and induces dramatic changes in the jet label ratios computed for Herwig++. This is a problem which must be addressed for use of this algorithm in fully-dressed hadron collider event simulations, and studies are underway to improve the robustness to MPI contamination. The exact reason for Herwig++’s extreme labelling susceptibility to MPI effects is not yet known. Changing the jet-label matching criteria to reject matches from label partons much softer than the particle jet will address some issues, and it is possible that suppressing flavour-changing clusterings with very soft quarks – as in the flavour- k_T clustering algorithm – may be an effective MPI rejection heuristic.

The code implementation of this algorithm, available in the FastJet contrib repository as `QCDAware`, allows for flexible “hybrid” approaches such as QCD-aware k_T reclustering of labelling partons selected by association to anti- k_T particle jets, for increased consistency with LHC experiment procedures.

It remains to be seen whether there is substance to hints that the labelling results may slightly overestimate the rate of quark jets. This is quite conceivable since pseudojet quark labels, once acquired, are harder to lose than gluon labels are: overlay of quarks from MPI can easily switch the label of an aligned hard-process gluon jet. This is a clear area for further investigation, in which the most obvious step is to introduce flavour- k_T style extra weighting for quark & gluon kinematics, as well as including the effects of different colour and EM charges, and the relative (running) strengths of the QED and QCD couplings. These extensions provide a clear motivation to focus on the k_T measure as the canonical distance choice for QCD-aware labelling.

Finally, we note that the inclusion of leptons and photons in the QCD-aware combination rules provides an attractive way to define truth-level dressed leptons and isolated photons in addition to jets, without overlaps or false distinctions between e.g. hard and “fragmentation” photons. Thus it may offer an appealing alternative truth object definition scheme to those already on the market [19]. There is perhaps also the possibility to extend the QCD-aware scheme with further

processes such as EW resonance decays which (like for partons) may not be reliably encoded in shower generator records: e.g. $\bar{q}_u q'_d \rightarrow W^-$ and $Wb \rightarrow t$ clusterings could be added with appropriate clustering weights. However, as the kinematics of these processes are non-Sudakov, there is no guarantee that they would work optimally, or even at all.

Acknowledgements

Our thanks to Donatas Zaripovas for his early work on testing the behaviour of the QCD-aware algorithm, to Gavin Salam for clarifying our questions about the impact and necessity of flavour- k_T distance measure modifications, and to Jesse Thaler for feedback on a draft version of this paper. And of course to the FastJet team for providing such a useful tool and their “contrib” repository for collecting community contributions such as the code described here.

References

- [1] S. Frixione, P. Nason, and C. Oleari, *Matching NLO QCD computations with Parton Shower simulations: the POWHEG method*, JHEP **0711** (2007) 070, arXiv:0709.2092 [hep-ph].
- [2] T. Gleisberg, S. Hoeche, F. Krauss, M. Schonherr, S. Schumann, et al., *Event generation with SHERPA 1.1*, JHEP **0902** (2009) 007, arXiv:0811.4622 [hep-ph].
- [3] S. Schumann and F. Krauss, *A parton shower algorithm based on Catani-Seymour dipole factorisation*, JHEP **0803** (2008) 038, arXiv:0709.1027 [hep-ph].
- [4] T. Sjöstrand, S. Mrenna, and P. Skands, *PYTHIA 6.4 physics and manual*, JHEP **05** (2006) 026, arXiv:hep-ph/0603175.
- [5] T. Sjöstrand, S. Mrenna, and P. Z. Skands, *A Brief Introduction to PYTHIA 8.1*, Comput.Phys.Commun. **178** (2008) 852–867, arXiv:0710.3820 [hep-ph].
- [6] T. Sjöstrand, S. Ask, J. R. Christiansen, R. Corke, N. Desai, et al., *An Introduction to PYTHIA 8.2*, Comput.Phys.Commun. **191** (2015) 159–177, arXiv:1410.3012 [hep-ph].
- [7] G. Corcella et al. JHEP **01** (2001) 010, hep-ph/0210213.
- [8] M. Bahr, S. Gieseke, M. Gigg, D. Grellscheid, K. Hamilton, et al., *Herwig++ Physics and Manual*, Eur.Phys.J. **C58** (2008) 639–707, arXiv:0803.0883 [hep-ph].
- [9] A. Banfi, G. P. Salam, and G. Zanderighi, *Infrared safe definition of jet flavor*, Eur.Phys.J. **C47** (2006) 113–124, arXiv:hep-ph/0601139 [hep-ph].

- [10] G. P. Salam, *Towards Jetography*, Eur.Phys.J. **C67** (2010) 637–686, arXiv:0906.1833 [hep-ph].
- [11] M. Cacciari, G. P. Salam, and G. Soyez, *FastJet User Manual*, Eur.Phys.J. **C72** (2012) 1896, arXiv:1111.6097 [hep-ph].
- [12] D. E. Soper and M. Spannowsky, *Finding physics signals with shower deconstruction*, Phys.Rev. **D84** (2011) 074002, arXiv:1102.3480 [hep-ph].
- [13] M. Dobbs and J. B. Hansen, *The HepMC C++ Monte Carlo event record for High Energy Physics*, Comput.Phys.Commun. **134** (2001) 41–46.
- [14] A. Buckley, J. Butterworth, L. Lonnblad, D. Grellscheid, H. Hoeth, J. Monk, H. Schulz, and F. Siegert, *Rivet user manual*, Comput. Phys. Commun. **184** (2013) 2803–2819, arXiv:1003.0694 [hep-ph].
- [15] M. Cacciari and G. P. Salam, *Pileup subtraction using jet areas*, Phys.Lett. **B659** (2008) 119–126, arXiv:0707.1378 [hep-ph].
- [16] D. Adams, A. Arce, L. Asquith, M. Backovic, T. Barillari, et al., *Towards an Understanding of the Correlations in Jet Substructure*, arXiv:1504.00679 [hep-ph].
- [17] A. J. Larkoski, J. Thaler, and W. J. Waalewijn, *Gaining (Mutual) Information about Quark/Gluon Discrimination*, JHEP **1411** (2014) 129, arXiv:1408.3122 [hep-ph].
- [18] ATLAS Collaboration, *Jet energy measurement with the ATLAS detector in proton-proton collisions at $\sqrt{s} = 7$ TeV*, Eur.Phys.J. **C73** (2013) no. 3, 2304, arXiv:1112.6426 [hep-ex].
- [19] ATLAS Collaboration, *Proposal for truth particle observable definitions*, Tech. Rep. ATL-PHYS-PUB-2015-013, CERN, Geneva, May, 2015.
<https://cds.cern.ch/record/1700541>.

A Further performance plots

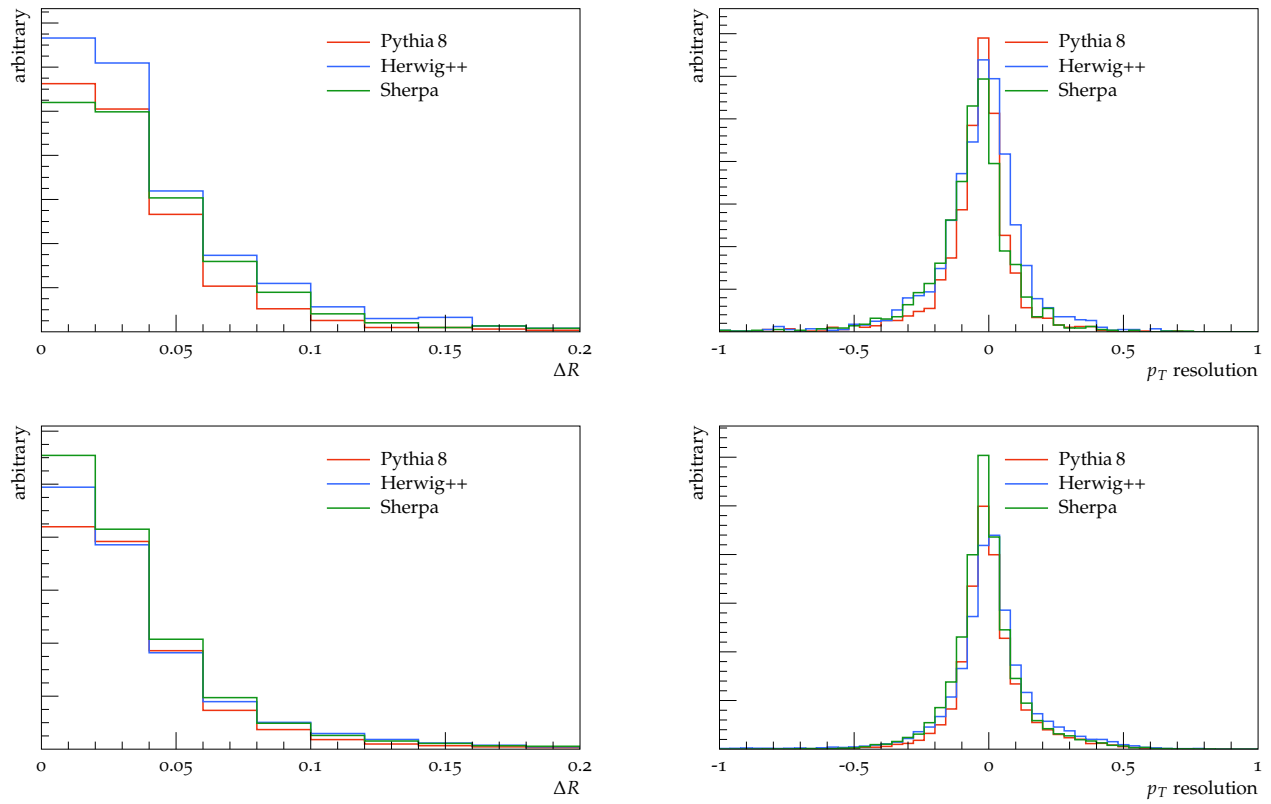


Figure 9: Heavy tagging performance/comparisons: γ + jet events, with bottom-labelled jets on the top row, and charm-labelled jets on the bottom row.

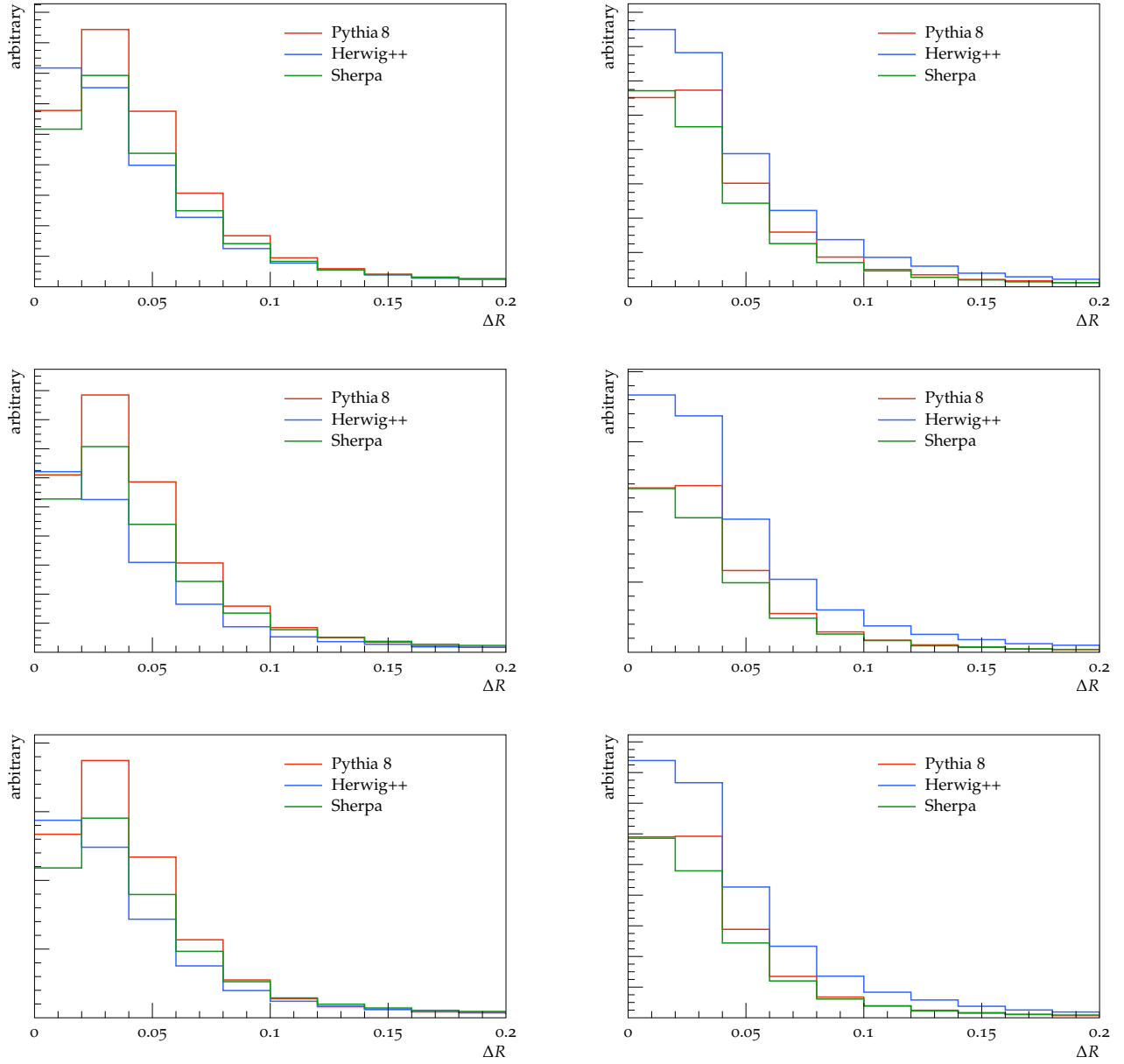


Figure 10: ΔR performance comparisons for gluon- (left) and light quark-labelled jets (right) in inclusive jet events, showing k_T labeled jets on the top row, anti- k_T in the middle, and k_T -reclustered on the bottom.

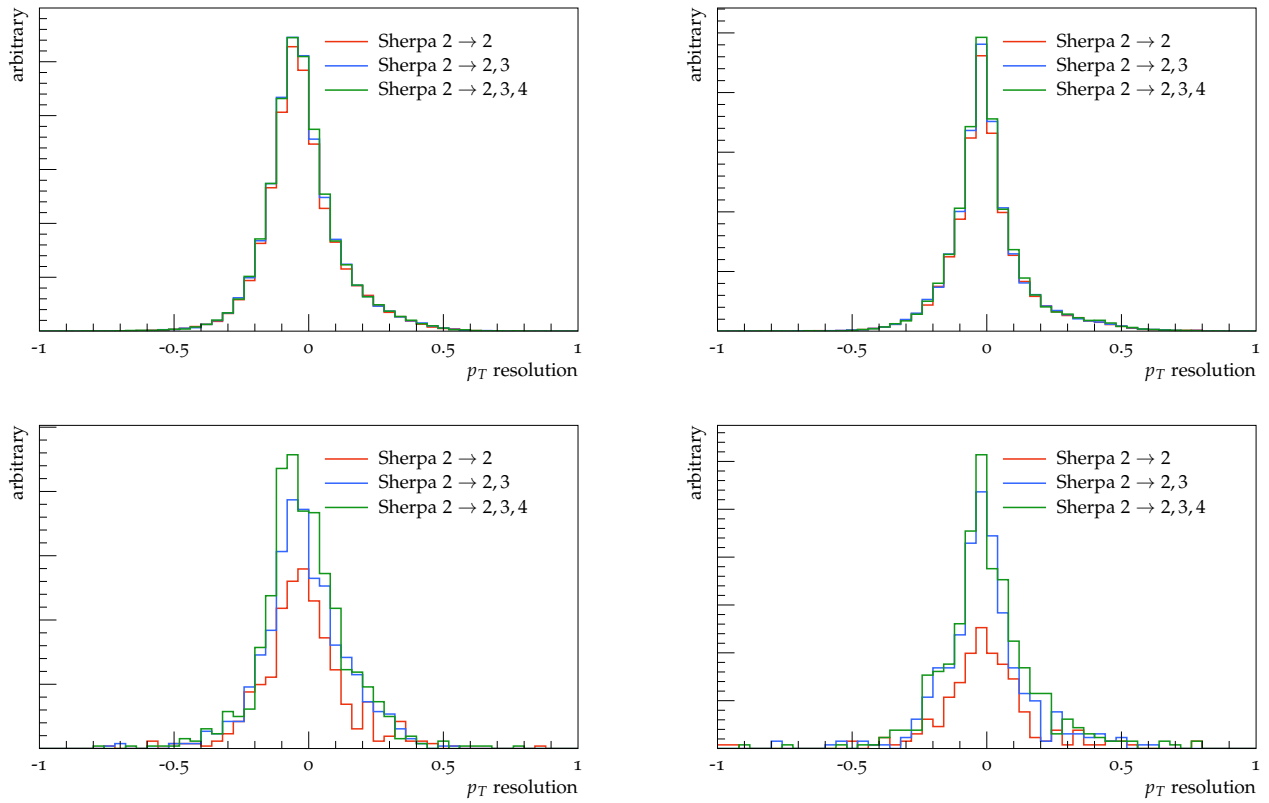


Figure 11: Jet labelling dependence on maximum number of ME partons in jet events for gluon- (left) and light quark-labelled jets (right). The top row shows all jets inclusively, the bottom only for the 3rd jet.